Behavior of Concrete-Filled FRP Tubes Under Bending, Axial Loads, and Combined Loading

Amir Fam, Bart Flisak and Sami Rizkalla

ABSTRACT

Innovative hybrid systems such as the concrete-filled fiber reinforced polymer (FRP) tubes are effective in facing the great demand for non-corrosive and durable piles, power transmission poles, highway overhead sign structures and bridge components. A three-phase experimental and analytical study was undertaken to examine the behavior of concrete-filled FRP tubes under pure bending, pure axial load, and combined loading in order to establish the axial load-bending moment interaction diagrams. This paper summarizes the findings of the experimental and the analytical studies, which are developed to provide guidance for design of concrete-filled FRP tubes.

INTRODUCTION

The concrete-filled glass-FRP cylindrical tube structural system has been investigated and found to be utilizing the characteristics and properties of the individual components effectively [1]. The FRP tube provides lightweight permanent formwork as well as non-corrosive reinforcement for the concrete, which simplify the construction and reduce erection time. The round tube also confines the concrete in compression and increases its strength and ductility, while the concrete core supports the tube and prevents premature local buckling failure. Structural applications of concrete-filled FRP tubes include piles, overhead sign structures, and poles as well as bridge girders and piers [2]. The FRP tubes are fabricated using the filament winding technique, which is capable of providing fibers in several directions. The fibers in the circumferential direction are utilized to provide confinement of the concrete, while the fibers in the axial direction provides the flexural strength and stiffness.

Amir Fam, Post –Doctoral Research Associate, NC State University, Raleigh, NC 27695-7533. E-mail: afam@unity.ncsu.edu
Bart Flisak, M.Sc. Student, University of Manitoba, MB, Canada R3T 5V6
Sami Rizkalla, Distinguished Professor of Civil Engineering and Construction, NC State University, Raleigh, NC 27695-7533

EXPERIMENTAL PROGRAM

The experimental program included testing of four beams in bending, three stubs under axial compression, and nine specimens under combined bending and axial compression loads. Five different GFRP tubes were used in this investigation. Table I provides the details of the tubes including diameter, thickness, fiber and matrix types, stacking sequence of different layers and mechanical properties of the tubes in the axial and hoop directions. Table II shows the characteristics of test beams, including the cross-section configurations, span, spacing between loads, tube identification number based on Table I, and the concrete strength. Tables III and IV provide similar details of the stubs and the beam-column specimens respectively.

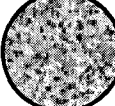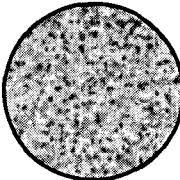## TABLE I. DIMENSIONS AND DETAILS OF THE GFRP TUBES

Tube #	Outer Diam. (mm)	Thickness* total (mm)	Thickness* structural (mm)	Fiber / matrix	Fiber volume % age	# of layers	Laminate structure and stacking sequence** Layer / thickness / angle 1	2	3	4	5	6	7	8	9	10	Axial direction f_u ten. MPa	comp. MPa	E GPa	υ	Hoop direc. f_u ten. MPa	E GPa
1	219	3.7	2.21	E-glass / epoxy	51	9	t (mm) 0.23 / θ (deg) +15	0.23 -82	0.23 -82	0.25 +15	0.25 -82	0.28 +15	0.25 -82	0.24 +15	0.25 -82		201	183	20	0.05	548	33.4
2	326	7.05	6.4	E-glass / epoxy	51	10	0.56 -88	0.43 +3	0.56 -88	0.56 -88	0.89 +3	0.56 -88	0.86 +3	0.56 -88	0.86 +3	0.56 -88	345~	276~	17	0.11	465#	24#
3	320	7.22	5.96	E-glass / polyester	51	5	1.04 +34	1.04 -34	1.8 +80	1.04 +34	1.04 -34						207~	103#	15	0.57	326#	17#
4	626	6.68	5.41	E-glass / polyester	51	5	0.94 +34	0.95 -34	1.63 +85	0.94 +34	0.95 -34						207~	103#	14	0.49	353#	18#
5	942	10.2	8.93	E-glass / polyester	51	7	1.14 +34	1.15 -34	2.07 +86	1.14 +34	1.15 -34	1.14 +34	1.14 -34				207~	103#	15~	0.39	216#	15#

* Some tubes have a liner at the inner surface to facilitate removing the tubes from the mandrel. The liner is not part of the structural wall thickness

** Angles of fibers are measured with respect to the longitudinal axis of the tube

~ Manufacturer data
# Lamination theory

TABLE II. DETAILS OF BEAMS

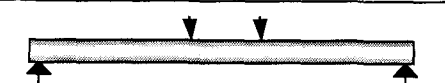| Beam no.	Span (m)	Spacing between loads (m)	Tube from Table 1	Config.	f_c' (MPa)
B1	5.5	1.5	2		60
B2	5.5	1.5	3		67
B3	5.0	1.5	4		33
B4	10.4	1.5	5		58

TABLE III. DETAILS OF STUBS
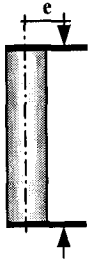
Stub no.	Config.	Diam. (mm)	Height (mm)	Tube from Table 1	f_c' (MPa)
C1		219	438	1	58
C2		219 / 95	438	1	58
C3		219 / 133	438	1	58

TABLE IV. DETAILS OF BEAM-COLUMNS

Spec. no.	height (m)	Tube from Table 1	e (mm)	f_c' (MPa)	Configuration	Test setup
BC1			30			
BC2			100			
BC3	1.8	2	200	60		
BC4			300			
BC5			10			
BC6			30			
BC7	1.75	3	100	67		
BC8			200			
BC9			300			

Fabrication of Specimens

The tubes used to fabricate the specimens were placed in an inclined position as shown in Fig. 1 and concrete was cast from top. The central holes in stubs 2 and 3 were achieved using cardboard tubes. The concrete mix was designed to provide pressure fit to the tubes by adding an expansive agent in order to prevent separation due to shrinkage. The stubs and beam-column specimens were cut from the concrete-filled tubes using a diamond saw as shown in Fig. 2.
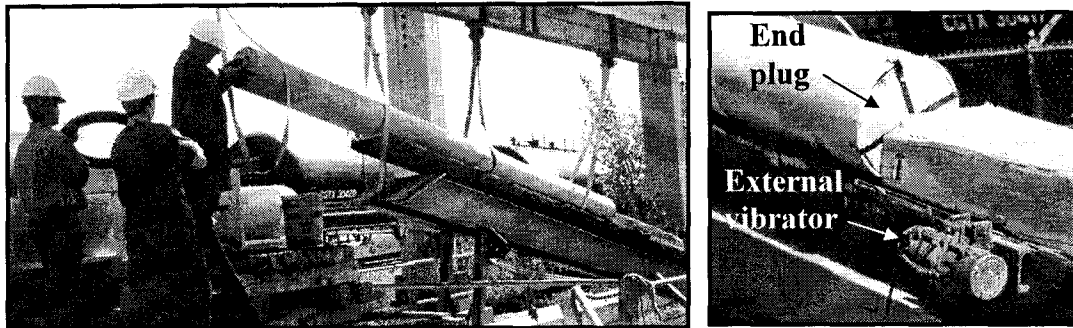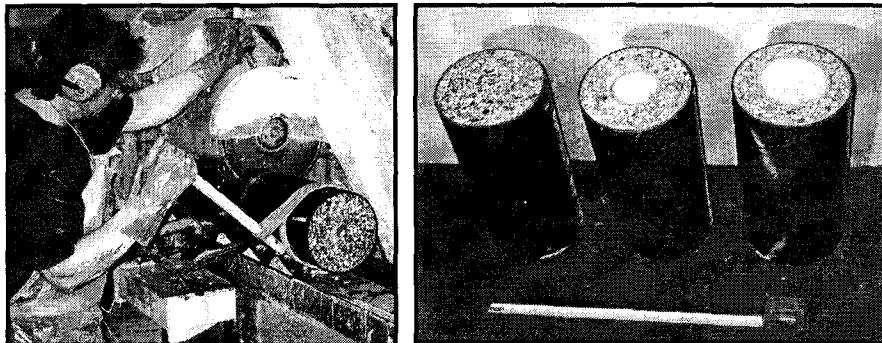

Figure 1. Casting setup of GFRP tubes

Figure 2. Cutting the stubs using a diamond saw

Beam Tests

Fig. 3(a) shows a typical test set-up for beams tested in bending using stroke control and four-point load configuration. Table II provides the specific details of the beams. Beams 1 and 2 are similar in size but have two different laminate structure of the FRP tube. Beams 2, 3 and 4 have similar laminate structure but different diameter-to-thickness ratios, which provided reinforcement ratios of 7.4, 3.5 and 3.8 percent respectively. In this paper, the reinforcement ratio ρ is defined as the ratio of four times of the thickness t and the diameter D, $(4t/D)$.

Stub Tests

Fig. 3(b) shows a typical test set-up for stubs under axial compression using stroke control. Details of the stubs are given in Table III. Axial and lateral strains were measured at four points around the perimeter. Stub 1 is totally filled with concrete, while Stubs 2 and 3 have central holes of different sizes.

Beam-Column Tests

Fig. 3(c) shows a typical test setup for the beam-column specimens. Table IV provides the details of the specimens. A rigid steel cap was used to apply the axial compression loads at different eccentricities. For a given eccentricity, the load was applied continuously up to failure. The combination of axial load and bending moment at ultimate was used to establish the interaction diagram. The pure flexural strength was obtained using the beam tests for Beams 1 and 2 of the same concrete-filled tubes.
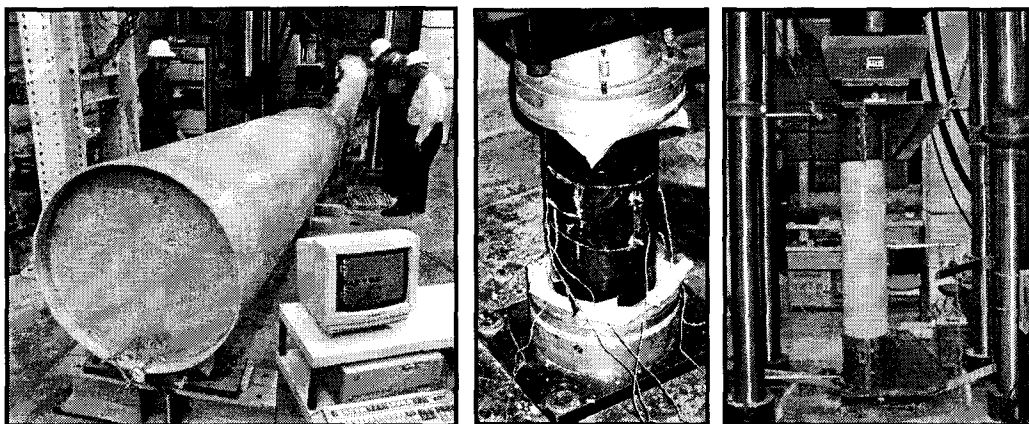
(a) Beam tests   (b) Stub tests   (c) Beam-column tests

Figure 3. Test setup of beams, stubs, and beam-columns

TEST RESULTS

Beam Tests

Fig. 4 shows the load-deflection behavior of Beams 1 and 2. The GFRP tubes (2 and 3) used for those beams had different laminate structure, which resulted in effective elastic moduli of 17 and 15 GPa in the axial direction respectively. The behavior suggests that the stiffness after cracking is almost proportional to the elastic moduli of the tubes. Analytical model, developed by the authors, based on equilibrium, strain compatibility and material properties [3], is used to predict the behavior of the beams as shown in Fig. 4. Good agreement is observed and the model is used in a parametric study as presented in a following section.
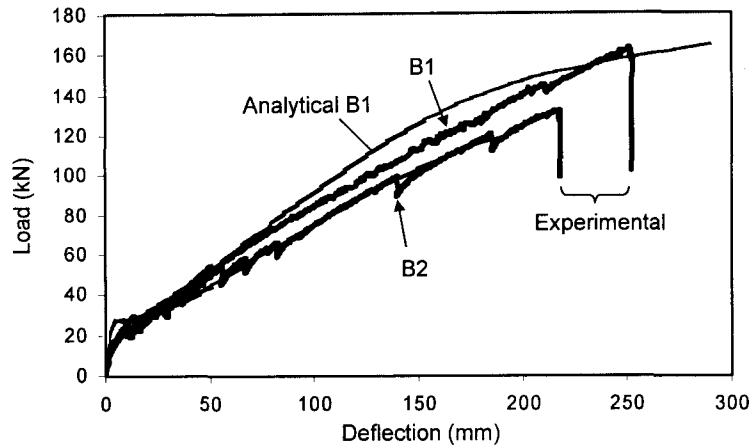
Figure 4. Load-deflection behavior of Beams 1 and 2

The behavior of Beams 2, 3, and 4 is compared using moment-curvature response, as shown in Fig. 5, due to the difference in span of the beams. The behavior is also normalized with respect to the diameter for comparison [4]. Curvatures are obtained using the measured strains. The normalized behavior of Beams 3 and 4
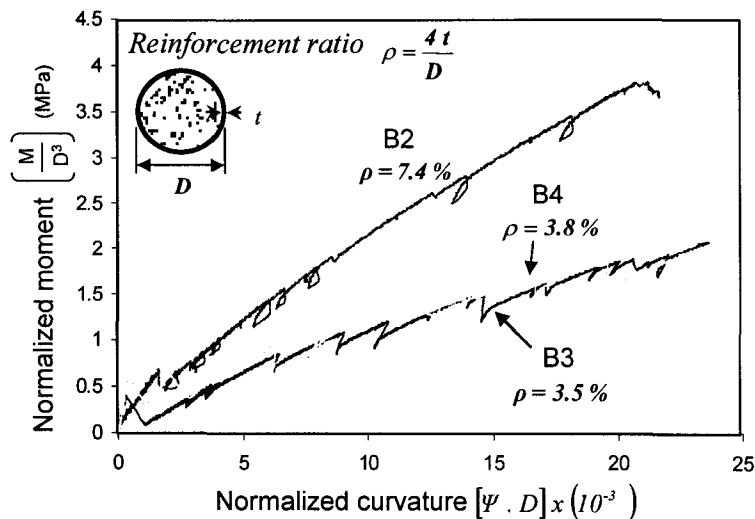
Figure 5. Normalized moment-curvature response of Beams 2, 3, and 4

are almost identical due to the similar reinforcement ratios, 3.5 and 3.8 percent respectively. Beam 2 showed higher strength and stiffness due to the higher reinforcement ratio of 7.4 percent. All beams failed in tension by rupture of fibers as shown in Fig. 10(a).

Stub Tests

Fig. 6 shows the measured and predicted stress-strain response of the confined concrete of Stubs 1 (totally filled with concrete), and Stubs 2 and 3 (with central holes of different sizes). The behavior shows increase of the strength and ductility of concrete due to confinement of the tube. The gain in strength in this case is low due to the low stiffness of the GFRP tube. It is also evident that providing a central hole reduces the confinement effect. In large diameter piles, central holes are used, however, to reduce the self-weight. A confinement model based on equilibrium and radial displacement compatibility between the outer shell and the concrete core is developed and accounts for the continuously increasing confining pressure due to the linear material properties of the tube [5]. The model shows good agreement with test data and is used in a parametric study as demonstrated in a following section. The stubs failed by fracture of the tube under combined hoop tensile stresses and axial compression stresses as shown in Fig. 10(b).
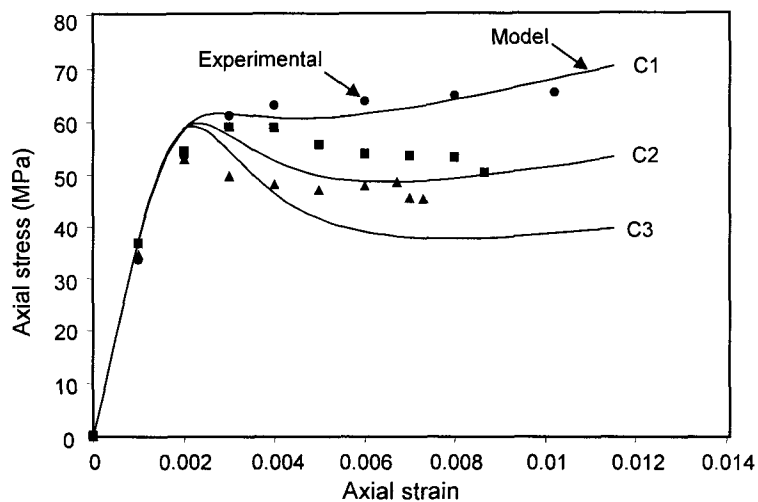

Figure 6. Stress-strain behavior of Stubs 1, 2 and 3

Beam-Column Tests

For beam-column specimens, the bending moment at ultimate was estimated based on the ultimate axial load and the eccentricity, which includes the initial eccentricity and the lateral deflection at mid height. The ultimate moment and axial load as well as the ultimate moments from the beam tests were used to establish the interaction diagrams for the two types of beam-column specimens (using GFRP tubes 2 and 3) as shown in Fig. 7. Tests are currently in progress to obtain data points near the axial strength of the specimens. Fig. 7 clearly shows the balanced points for the

two types of specimens, where the tension and compression failures occur simultaneously.
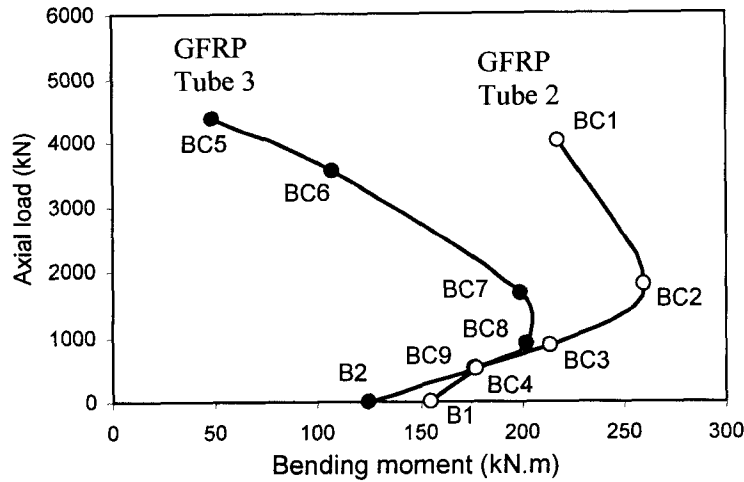

Figure 7. Interaction diagrams of the beam-column specimens

Fig. 8 shows the moment-curvature response of BC1 and BC6 with the two different GFRP tubes. Both specimens are tested using 30 mm eccentricity. BC1 shows higher flexural strength and stiffness due to the higher tensile strength and modulus of the tube in the axial direction as well as the better confinement effect of tube 2. Fig. 9 shows the axial load versus maximum axial compressive strain for BC1 and BC6. The higher axial strength of BC1 is mainly due to the lower Poisson's ratio of tube 2, which results in less separation of the tube from the concrete core and therefore provides higher level of confinement. Also, tube 2 has higher stiffness in the hoop direction, which improves the confinement effect.
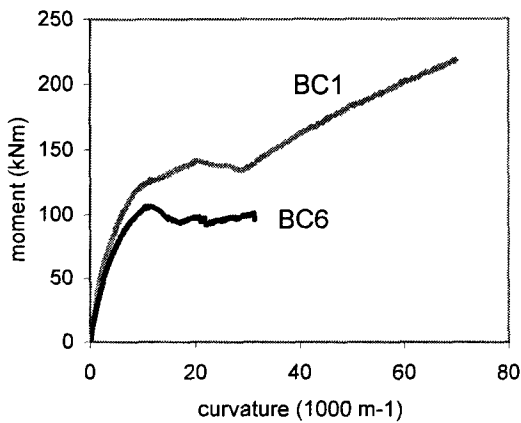

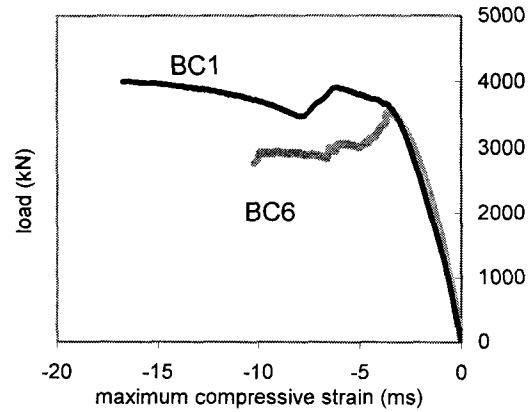Figure 8. Moment-curvature response   Figure 9. Load-strain response

Fig. 10 (c and d) shows a sample of compression and tension failure modes of specimens using GFRP tubes 3 and 2 respectively. Tension failure occurred by

rupture of the GFRP tube, while compression failure occurred by crushing of the tube.

(a) Beams   (b) Stubs   (c) Beam-col.(tube 3) (d) Beam-col.(tube 2)
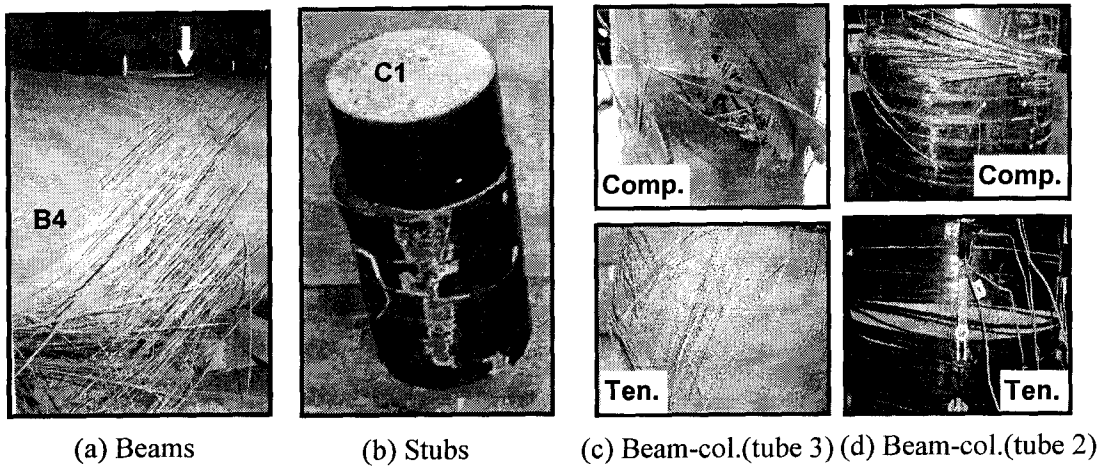
Figure 10. Different failure modes

PARAMETRIC STUDY

Beams

The analytical model was used in a parametric study to examine the effect of laminate structure and thickness of the tube. A 300 mm diameter GFRP tube with a $[0/90]_s$ symmetric cross ply E-glass/epoxy laminate is used in the analysis. The laminate structure is changed by varying the proportions of fibers in the axial [0] and hoop [90] directions including 9:1, 3:1, 1:1, and 1:3 ratios respectively. A 3:1 laminate indicates that 75 percent of fibers is oriented in the axial direction. The different proportions resulted in effective elastic moduli and tensile strengths of 35.2 to 11.5 GPa and 976 to 319 MPa respectively in the axial direction. The wall
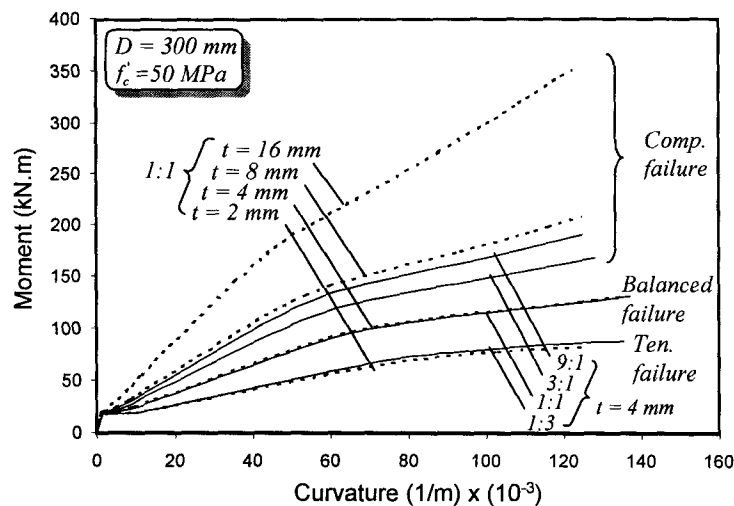

Figure 11. Effect of laminate structure and wall thickness on flexural behavior

thickness varied from 2 to 16 mm, which is equivalent to reinforcement ratios of 2.67 to 21.33 percent. Fig. 11 shows that increasing either the wall thickness for a given laminate structure, in this case (1:1), or increasing the ratio of fibers in the axial direction for a given wall thickness, in this case 4 mm, have a similar effect, which is increasing the flexural strength and stiffness of the member. The failure mode could however change from tension failure for lower stiffness or thin tubes to compression failure for higher stiffness or thick tubes.

Columns

The confinement model was used to examine the effect of the stiffness of the tube in both the hoop and axial directions under two loading conditions, as well as the effect of central hole size. For this study, a typical 150 mm diameter concrete-filled GFRP tube using 40 MPa concrete with 0.002 strain at peak unconfined strength and 0.18 initial Poisson's ratio, is axially loaded. Two extreme laminate structures were considered for the GFRP tube, including all fibers oriented in the hoop direction [90], or all fibers oriented in the axial direction [0], in order to provide the maximum and minimum stiffness in both directions. This parameter was studied for a GFRP tube of 2 mm thickness. The E-glass/epoxy GFRP tube has a 55 percent fiber volume fraction. The major and minor elastic moduli are 39 and 8.6 GPa and the major and minor Poisson's ratios are 0.28 and 0.06, respectively. The effect of tube thickness was studied for the case of fibers oriented in the hoop direction by varying the thickness from 0.5 mm to 8 mm. The effect of hole size was considered by varying the diameter of the central hole from zero (totally filled tube) to 125 mm for the case of the 2 mm GFRP tube with maximum stiffness in the hoop direction [90]. Fig. 12 shows the variation of the strength of confined concrete f_{cc}', normalized with respect to the unconfined strength f_c', with the stiffness of the tube in the hoop direction (Et/R), where R and t are the radius and thickness of the FRP tube respectively, and E is the elastic modulus of the tube in the hoop direction. The figure also shows the variation of the confined strength ratio (f_{cc}'/f_c') with the inner-to-outer diameter ratio (D_i/D_o). The figure indicates that increasing the stiffness of the tube in hoop direction would increase the strength
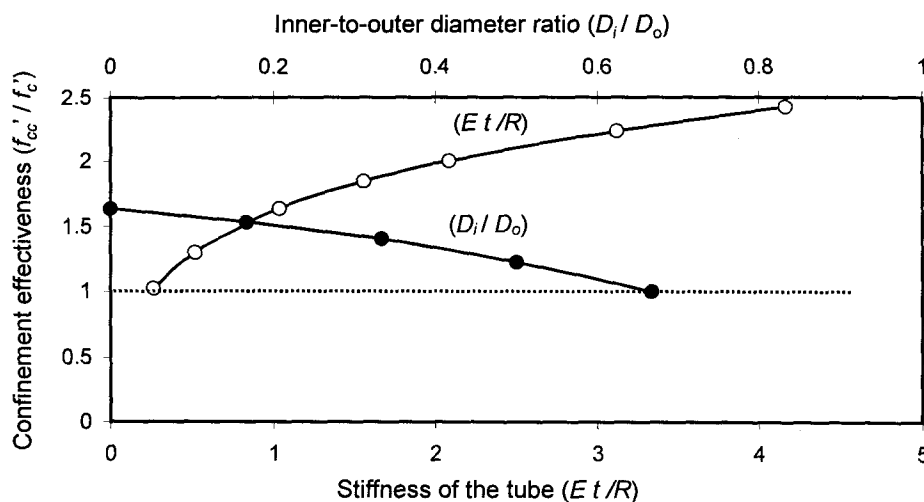

Figure 12. Effect of stiffness of the tube and inner hole size on confinement

of confined concrete, however, the rate of increase is nonlinear. The figure also shows that below a certain stiffness level, there is no gain in strength, due to the post-peak softening behavior. Also, increasing the size of the inner hole would reduce the confinement effect.

Fig. 13 shows the confined stress-strain behavior of concrete using a 2 mm GFRP tube. The behavior is given for the [90] laminate where all fibers are oriented in the hoop direction for maximum hoop stiffness and minimum axial stiffness, and the [0] laminate with all fibers in the axial direction. For each laminate, the load was applied either to the concrete core only, or to both the core and the tube. When the load is applied to the core only, the tube is fully utilized in the hoop direction and develops the full strength. In this case the [90] laminate provides maximum gain in the strength due to its high tensile strength and modulus, 1080 MPa and 39 GPa, respectively, whereas the [0] laminate is less effective due to its lower strength and stiffness in the hoop direction, 39 MPa and 8.6 GPa, respectively. When the load is applied to both the core and the tube, significant reduction in performance in terms of both strength and stiffness is observed, especially in the [90] laminate. The reduced strength is attributed to the bi-axial state of stress developed in the tube. The reduced stiffness is attributed to the outward expansion of the tube due to its Poisson's ratio effect, which reduces the confining pressure. In this regard the [90] shows a smaller reduction due to its smaller Poisson's ratio, 0.06, compared to the 0.28 of the [0] laminate.
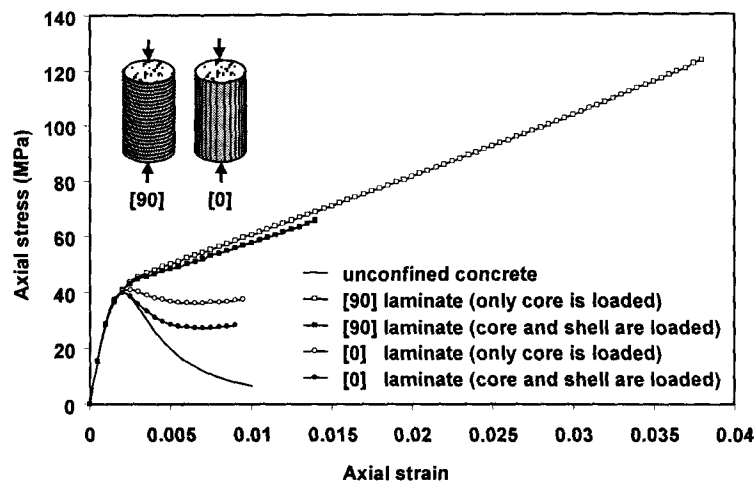

Figure 13. Effect of fiber orientations and loading conditions

CONCLUSIONS

1. Load-deflection behavior of beams using concrete-filled GFRP tubes is almost bi-linear with cracking load is small compared to ultimate load. Stiffness after cracking is governed by the laminate structure and diameter-to-thickness ratio of the tube.

2. Concrete-filled FRP tubes with thicker walls or higher percentage of fibers in axial direction, subjected to bending, tend to fail in compression.

3. A strain compatibility/equilibrium model using the effective mechanical properties of FRP tube in axial direction and unconfined concrete properties predicts well the flexural behavior of concrete-filled FRP tubes.

4. Increasing the wall thickness of FRP tubes or orienting the fibers as close as possible to the hoop direction increases the confinement effect under axial compression, while increasing the central hole size reduces the confinement.

5. Ignoring the effect of axial loading of the tube under compression overestimates the confinement effect. The tube is bi-axially loaded under axial compressive and hoop tensile stresses, which reduces its hoop strength.

6. A confinement model has been developed and accounts for totally filled tubes or tubes with central holes, as well as axial load applied to both the concrete and FRP tubes. The model predicts well the stress-strain response of FRP confined concrete.

7. The axial load-bending moment interaction diagram of concrete-filled FRP tubes is similar to conventional reinforced concrete members. In the initial stage, as axial load increases, moment capacity increases and failure is governed by rupture of the FRP at tension side. A balanced point is reached, where the curve reverses direction, and moment capacity decreases with increasing axial load, where failure is governed by crushing of the FRP at the compressive side.

REFERENCES

1. Mirmiran, Amir and Shahawy, Mohsen. (1997). "Behavior of Concrete Columns Confined by Fiber Composites," *Journal of Structural Engineering,* May, pp. 583-590.

2. Seible, Frieder. (1996). "Advanced composites materials for bridges in the 21st century," Proceeding of the First International Conference on Composites in Infrastructure (ICCI'96), Tucson, Arizona, Jan., pp. 17-30.

3. Fam, Amir Z. (2000). "Concrete-Filled Fiber Reinforced Polymer Tubes For Axial and Flexural Structural Members," Ph.D. Thesis, The University of Manitoba, pp. 261.

4. Park, R., and Paulay T. (1975). "Reinforced Concrete Structures," Ed. by John Wiley & Sons.

5. Fam, Amir Z. and Rizkalla, Sami H. (2001). *"Confinement Model for Axially Loaded Concrete Confined by FRP Tubes"*, ACI Structural Journal, ACI Structural Journal, Vol.98, NO.4, July-August.